Computational Sciences and Engineering 5(2) (2025) 245-265

University of Guilan

Computational Sciences and Engineering

journal homepage: https://cse.guilan.ac.ir/

Simulation of fluid flow in a counter-flow heat exchanger with partly elastic intermediate walls

Seyed Esmail Razavi[a,*], Tohid Adibi [b,*]

[a] Department of Mechanical Engineering, University of Tabriz, Tabriz, Iran
[b] Department of Mechanical Engineering, University of Bonab, Bonab, Iran

ARTICLE INFO

Article history:
Received 25 December 2025
Received in revised 9 February 2026
Accepted 10 February 2026
Available online 10 February 2026

Keywords:
Heat exchanger
Counterflow
Oscillating elastic plate
Oscillating number
Cold temperature
Cold outlet

ABSTRACT

Heat exchangers are a major component of many heat-related systems, and improving their heat transfer efficiency is a significant engineering challenge. Though the problems of geometric optimization and vibration-assisted mechanisms have been widely discussed, little has been done to examine the impact of partly elastic intermediate walls and oscillatory behavior in counter-flow configurations. This paper numerically simulates the fluid flow and heat transfer in a counter-flow plate heat exchanger with partially elastic intermediate walls with a fully coupled fluid-structure interaction (FSI) methodology. The thermal and hydrodynamic performance of an elastic wall location, oscillation mode, frequency, and amplitude are analyzed. They indicate that the proposed configurations are highly effective in promoting heat transfer, where the increase in Nusselt number is between 23% and 83% in the optimal mid-uniform oscillation scenario. When the oscillation frequency changes to 3 Hz, the Nusselt number is increased by as much as 48 percent, indicating that oscillating elastic walls have a great potential in enhancing heat transfer. Considering the importance of the overall thermo-hydraulic performance (PEC), the performance evaluation criterion was also calculated, confirming that the optimal configurations provide a net performance benefit, with PEC values exceeding 1.0 and reaching up to 1.29.

1. Introduction

The heat exchangers are essential in a diverse range of applications in the engineering field, such as energy systems, chemical processing, HVAC installations, and thermal processing of electronic equipment[1-3]. Counter-flow heat exchangers, among other designs, are very popular because they have a high thermal efficiency and high heat transfer, unlike parallel-flow ones[4, 5]. The

* Corresponding author.
E-mail addresses: razavi@tabrizu.ac.ir (S.E. Razavi); tohidadibi@ubonab.ac.ir (T. Adibi)

https://doi.org/10.22124/cse.2026.31974.1132

predictability of the flow in such systems is crucial because it enhances the thermal performance, design parameters, and the reliability of the operations. Although classical analyses commonly assume immobile and hard walls, this may not be a sufficiently realistic model of real-world problems where structural flexibility, material compliance, or mechanical loading can cause wall deformation and a change of flow field.

Different strategies for enhancing industrial heat exchange performance have been comprehensively reviewed by Stehlík and Wadekar[6]. The study classifies the improvement methods into global and local intensification, whereby the former involves the best use of the heat exchanger network design to achieve maximum energy recovery, and the latter involves the improvement of the performance of single units. Conventional and advanced shell-and-tube heat exchangers, such as helically baffled designs, were investigated to demonstrate how the network level and unit level optimization techniques may be combined to achieve success. The efficiency improvement of miniaturized heat exchangers using passive enhancement techniques has been investigated by Gerken et al. [7]. Pin fin geometries of micro heat exchangers were investigated because it has high surface to volume ratios and short heat transfer distances. The experiment of the study experimentally measured the augmentation of heat transfer and the pressure losses, and used the overall exergy loss method as an evaluation tool to define the trade-off between a higher thermal performance and a higher flow resistance. The application of artificial intelligence techniques to enhance heat exchanger efficiency has been extensively analyzed by Lodhi et al. [8]. The performance optimization, diagnostics, and predictive maintenance were considered with machine learning, deep learning, and expert systems. The emergent solutions included hybrid AI solutions and smart heat exchangers with IoT facilities. Although they are promising, issues of data quality, computation cost, and system integration were expressed as major constraints that needed to be investigated. Methods for increasing thermal efficiency through the integration of heat exchangers with renewable energy sources and heat pumps have been reviewed by Osintsev et al. [9]. Different types of heat exchangers were covered, where analytical, experimental, and design-based methods were discussed with special reference to plate heat exchangers and optimization using software. The exergetic and energy balance techniques were used to assess the integrated energy technology complexes, such as desalination systems, emphasizing the avenue of enhancing the overall system performance.

Although a lot has been done using geometric optimization, advanced materials, and system-level integration, most existing studies remain rigid and stationary with respect to the heat exchanger walls. Nevertheless, the flexibility and elastic deformation of the wall in most practical applications may combine with the flow field, resulting in altered velocity distributions and possibly improved heat transfer[10, 11]. This has led to recent studies that have focused on the application of elastic or compliant walls as one of the active-passive mechanisms to enhance thermal performance. In that regard, an increasing amount of literature has been dedicated to fluid flow and heat transfer in systems with elastic surfaces. Adibi et al. [12] have numerically examined the influence of elastic walls regarding the thermal performance of counterflow heat exchangers through a fluid-structure interaction framework. Elastic plates were placed at various points in the exchanger, with external forces being applied to cause deformation. The findings showed that configurations of elastic plates performed much better than rigid designs, and efficiencies were increased up to 140%, and heat transfer rates were increased, especially when the plates were symmetrically arranged. Ji et al. [13] have numerically investigated the vibration and heat transfer of a conical spiral elastic tube bundle heat exchanger through the bidirectional fluid-solid coupling. A variety of designs of pulsating and non-pulsating baffles were studied in a large range of Reynolds numbers. It was found that schemes with baffles improved the regularity of flow, the amplitude of vibration, and the overall thermal performance, and the direction of installation of the baffles was also a key factor in the holistic promotion of heat transfer. In other work[14], they have numerically studied the heat transfer of elastic tube bundle heat exchangers with enhanced tube structures and segmental baffles. Several traditional and adapted designs, including and without baffles, were compared regarding vibration-enhanced heat transfer and pressure drop. These findings showed that structural modification and installation of baffles had a considerable positive effect on thermal performance, and the best thermohydraulic performance was observed with the improved elastic tube bundle with baffles.

Ji et al. [15]proposed two schemes for spiral elastic tube (SET) heat exchangers, same-direction deflector SET (SD-SET) and reverse-direction deflector SET (RD-SET), and investigates their vibration response and heat transfer capacity (HTC) using a bi-directional fluid-structure coupling method. The results show that the RD-SET heat exchanger has a higher overall HTC than the SD-SET heat exchanger, with a maximum increase of 43.28%, and that optimizing the RD-SET heat exchanger structure further improves its HTC by 0.49% and extends the fatigue life of the SET. The study finds that flow-induced vibration can effectively improve the HTC of SET, but a larger vibration amplitude does not necessarily result in a better HTC enhancement effect. Afridi et al. [16] performed some tests on a new heat exchanger experimentally. Adibi et al. [17] introduced a novel multi-twisted blade turbulator (MTBT) designed to enhance heat transfer in heat exchanger tubes by generating swirling and radial flows simultaneously. A comprehensive numerical analysis was conducted to evaluate the hydrothermal performance of the MTBT under various geometric parameters, leading to an optimal configuration that achieved a performance evaluation criterion (PEC) of 2.8. Xu et al. [18] investigated the thermal deformation and stress of a printed circuit heat exchanger (PCHE) with mini-channels, a key component in advanced nuclear reactor power generation systems, using homogenization and finite element analysis methods. The results show that the PCHE exhibits macroscopic thermal deformation and thermal stress concentration around the junctions between the core and cover plate, with different stress and strain patterns obtained from elastic and elastic-plastic analyses. The study recommends using elastic-plastic analysis instead of elastic analysis, particularly under strong constraint conditions, as it provides more accurate results, with relative deviations of stress and strain of up to 120.786% and 10.139%, respectively. Razavi et al. [19] used OpenFOAM to analyze the impact of key parameters, such as fluid flow rate, inlet humidity, and channel geometry, on heat transfer efficiency, finding that optimizing these parameters can significantly improve performance. The results provide valuable insights for engineers and researchers, offering practical guidance for sustainable cooling solutions and addressing global energy efficiency challenges, with parallel flow configurations showing up to 18% higher efficiency than counter-flow setups. Ji et al.[20] investigated the impact of baffle structural parameters on the vibration and heat transfer of elastic tube bundle (ETB) heat exchangers, using a bi-directional fluid-structure interaction calculation method. The results show that increasing the baffle height improves the comprehensive heat transfer performance (HTP) while suppressing vibration, with a maximum decrease in vibration amplitude of 10.05% and an increase in heat transfer coefficient of 5.50%. However, the baffle curvature has a positive effect on vibration-enhanced HTP, with an optimal curvature of 10° achieving maximum values for Nusselt number per unit pressure drop and performance evaluation criteria.

Although there has been an increased interest in elastic and vibration-assisted heat exchangers, most of the current studies are based on fully elastic tube bundles or uniformly deformable walls, and little thought has been given to the contribution of partly elastic intermediate walls and their spatial distribution in counter-flow configurations. Specifically, the interaction between the elastic wall location, oscillation mode, frequency, and amplitude, and their effect on the flow structure and heat transfer performance, is not sufficiently studied. To address this knowledge gap, the current paper numerically examines fluid flow and heat transfer in a counter-flow plate heat exchanger with partly elastic intermediate walls through a fully coupled fluid-structure interaction method. Elastic wall position and oscillatory nature are studied systematically to offer new information in designing high-performance heat exchangers.

2. Materials and methods

In this section, we will first examine the equations governing fluid flow, then discuss conventional methods for solving these equations, and finally introduce the solution geometry and boundary conditions of the problem. The governing equations of the problem in finite element form are as follows: $\int_{\Omega}(\nabla.U).qd\Omega=0$ $\int_{\Omega}(\nabla.U).qd\Omega=0$

$$\int_{\Omega}(\nabla.U).qd\Omega=0 \tag{1}$$

$$\int_{\Omega}(\frac{\partial U}{\partial t}+(U.\nabla)U-\frac{1}{\rho}\nabla p+\nu\nabla^{2}U).wd\Omega=0 \tag{2}$$

$$\int_{\Omega}(\frac{\partial T}{\partial t}+(U.\nabla)T-\alpha\nabla^{2}T).\phi d\Omega=0 \tag{3}$$

The above relations are the continuity, momentum, and energy equations, respectively. In the above equations, we have:

U: represents the velocity vector, which is a function of position and velocity.

P: represents the pressure field.

ρ : is the fluid density.

μ : is the kinematic viscosity.

∅ : is the heat dissipation

t: time

Ω: is the physical domain in which the problem is modeled.

T: represents the fluid temperature

In the finite element method, experimental functions are created to approximate the numerical solution of the partial differential equations. These functions are selected from a space with certain properties to satisfy the boundary conditions and provide a good approximation of the numerical solution. The ultimate governing equations of most FSI systems are: conservation of mass, momentum, fluid flow, coupled with conservation of momentum (Newton's second law) for solids, and mechanical equilibrium equations for solids. The unknown quantities of the flow equations include fluid pressure, components of the fluid's vertical velocity, solid deformation, and solid stress. To find these unknowns, additional equations are needed, called constitutive equations. They relate fluid forces to fluid motions and solid forces to deformations. These constitutive equations describe the properties of the fluid or solid and have a wide range of complexity. The governing equations of the fluid, solid, and lattice displacements are:

$$\frac{\partial U_i}{\partial x_i} = 0 \tag{4}$$

$$\rho_f\left[\frac{\partial U_i}{\partial x_i} + \left(U_j - U_j^m\right)\frac{\partial U_i}{\partial x_i}\right] = -\frac{\partial P}{\partial x_i} + \frac{\partial \tau_{ij}}{\partial x_j} + f_i^v \tag{5}$$

$$\tau_{ij} = \mu\left[\frac{\partial U_i}{\partial x_j} - \frac{\partial U_j}{\partial x_i}\right] \tag{6}$$

Eq. (4) is the fluid flow continuity equation. ***Eq. (5)*** is the momentum equation governing the fluid flow, where p is the fluid flow pressure, ρ is the fluid density, μ is the fluid viscosity, v is the fluid flow velocity vector, τ is the fluid shear stress tensor, and f is the physical force vector acting on the fluid domain. The shear stress tensor is the component of the force vector that is parallel to the cross-sectional area of the fluid element from the solid surface to the fluid element. To obtain the fluid shear stress, multiply the shear rate, which means the rate of change in velocity at which a fluid layer passes over its neighboring layer, by the dynamic viscosity of the fluid.

The structural laws of the solid domain and Hooke's law are as follows.

$$\frac{\partial \sigma_{ij}}{\partial x_j} + \rho_s f_i^{VS} = \rho_s \times a_i, a_i = \frac{dU_i}{dt} \tag{7}$$

$$\sigma_{ij} = C_{ijkl}E_{kl} \tag{8}$$

$$E_{ij} = \frac{1}{2}\left(\frac{\partial \mu_i^s}{\partial x_j} + \frac{\partial \mu_j^s}{\partial x_i}\right) \tag{9}$$

The symbols used in the above relationships are as follows.

f_i^v : Physical force vector acting on the fluid domain

σ_{ij} : Solid stress tensor, which defines the forces acting per unit area at a point in a material in a deformed state.

f_i^{VS} : Physical force vector acting on the solid domain

ρ_s : Solid density

a_i : Acceleration vector of the solid domain

C_{ijkl} : Stiffness matrix

u^s : Velocity in the solid part

E_{ij} : Lagrangian strain tensor

It is worth noting that the convective terms have the largest change in momentum conservation. The convective terms must consider the shape-changing mesh and its velocity. The general method is to use the diffusion transport equation to define the mesh displacement at any point in the control volume from end to end of the domain. The mesh displacement relative to previous mesh locations is a variable that is operated on by the slope and divergence operator and is a stiffness function that allows for uniform distribution of the displacement throughout the computational domain.

Often, the stiffness parameters are a function of the element control volume, allowing the mesh to have different stiffness values at different points in time for the analysis. Such a function is very important to prevent mesh folding and negative element volumes from forming during FSI analyses with large convective forces.

There are two primary [21]methods for linking solid and fluid domains. The first is a direct coupling method, where the solid and fluid physics are solved in a single computational step. The second is an iterative coupling method, where the solid and fluid physics are solved in a step-by-step process. This means that the fluid physics is solved first, and the fluid forces are fed as input to the solid physics simulation. Iterative coupling is used in most situations to control for nonlinearities in the fluid domains and to ensure that the physics is not lost during the coupling process. The friction coefficient in the flow inside the channel is obtained from the following equation [21].

$$f = \frac{\tau_w}{0.5\rho u_m^2} = \frac{\mu \frac{\partial u}{\partial y}}{0.5\rho u_m^2} \tag{10}$$

Where f is the friction factor, τ_w is the wall stress, ρ is the density, u_m is the mean velocity, μ is the viscosity. The Nusselt number in the flow inside the channel is obtained from the following equation [21].

$$Nu = \frac{hL_{ref}}{k} = \frac{\frac{k\frac{\partial T}{\partial y}L_{ref}}{(T_w - T_m)}}{k} = \frac{\frac{\partial T}{\partial y}L_{ref}}{(T_w - T_m)} \tag{11}$$

Where Nu is the local Nusselt number, h is the convective coefficient, L_{ref} is the channel wide, T_w is the wall temperature, T_m is the mean temperature, and k is the conductivity. In this study, the velocity and temperature gradients are obtained by a second-order numerical method, considering the velocity and temperature at the wall and subsequent points on the created grid.

In this research, to increase the heat transfer rate, a new heat exchanger has been designed and simulated, which will be described in more detail below. The investigated model is a counter flow plate heat exchanger with a square cross-section with a side length of 2 cm. The entire computational domain includes the general parts of the fluid domain with temperature boundary conditions, the solid domain, and the common boundary of the interaction of these two domains. Each of these three comprehensive parts has different subsets. The flowing fluid domain is the same water entering the exchanger from two separate inlets in different directions with different temperatures. The solid domain includes a part of the exchanger walls that is considered as an oscillating and half-sinusoidal domain with different frequencies at different locations. The boundary between the two domains includes the heat transfer operation between the two cold and hot fluids through the common plane between the two fluids that is being considered. ***Figures 1 and 2*** shows the details of the designed heat exchanger.

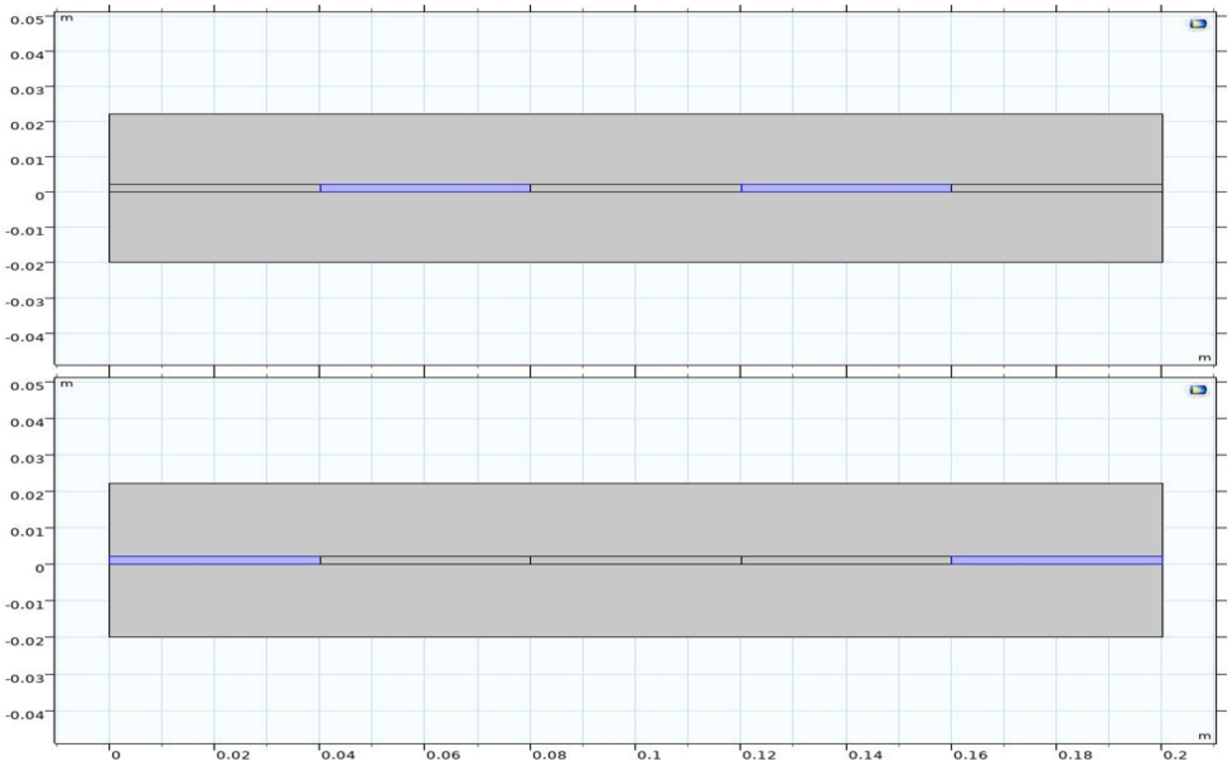

Figure 1. Problem geometry in two cases: middle and side elastic plates

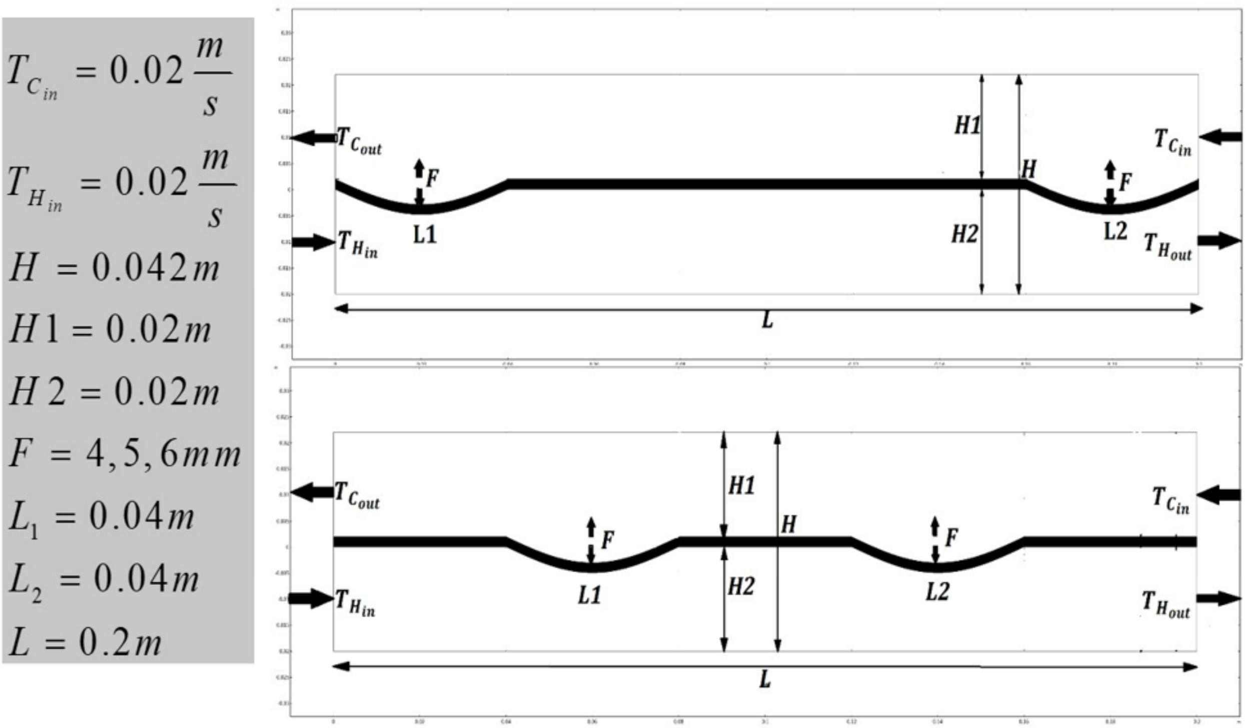

Figure 2. Problem geometry and boundary conditions

According to ***Figure 1***, hot fluid with a temperature of 330 K enters from the upper channel and cold water with a temperature of 300 K enters from the lower channel in opposite directions at a uniform velocity. All constant and temperature-dependent properties are considered by the software by assuming the fluid to be pure water, which is an incompressible, Newtonian, viscous fluid with a given dynamic viscosity at a velocity of 0.02 m/s and a Reynolds number of approximately 467 for the cold fluid and a Reynolds number of approximately 804 for the hot water. The oscillation frequency of the elastic part is 1, to 5 Hz in three cases, and the oscillation amplitude is also considered to be 4 and 5 mm. The geometric dimensions, temperature difference, and flow velocity were chosen to represent a typical laminar operating condition for compact plate heat exchangers. The oscillation frequency (1–5 Hz) and amplitude (4–5 mm) ranges were selected to ensure physically significant flow perturbation while maintaining numerical stability in the fully-coupled FSI simulation. The displacement equation of the oscillating part is also as follows: D is the oscillation amplitude, and F is the oscillation frequency. The meshing of the computational domain was done using Comsol Multiphysics. In this two-channel geometry, a triangular mesh (Free Triangular) with a maximum size of 1.5 mm was used. In the triangular mesh mode, the number of elements is 17396. And considering the clustering in the boundary layer section for greater accuracy in the solution, the mesh quality is approximately 85 percent. A sample mesh can be seen in ***Figure 3***.

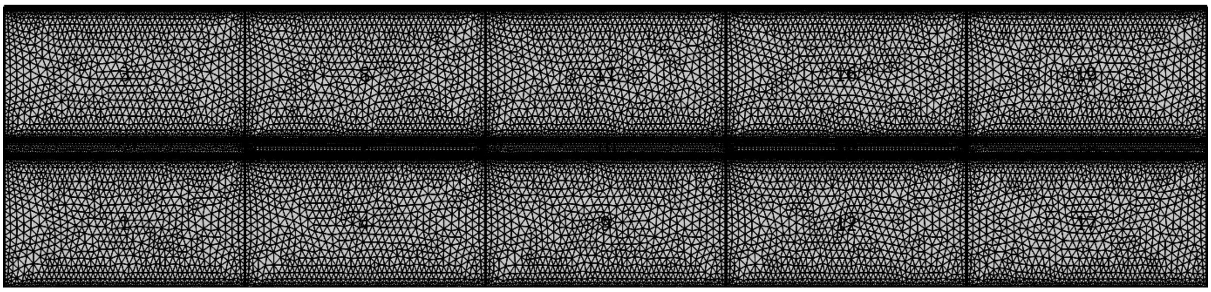

Figure 3. The generated mesh with clustering on solid boundaries

The elastic part of the wall consists of two elastic parts and two rigid parts, considering two cases: in the first case, the elastic walls are located in the middle section, and in the second case, they are located in the corner section. The wall material in the rigid part is copper with a density ρ of 8960 kg/m3, Young's modulus of 117 GPa, and Poisson's ratio of 0.35. The elastic part is made of copper cladding with a thickness of 0.5 mm, and in the middle is made of elastic material with a copper intermediate wall in the fixed parts with a specific heat of 35 kJ/kg.K and thermal conductivity of 400 W/m.K. The elastic parts are made of copper sheet cladding with a thickness of 0.5 mm and elastic material with thermal conductivity (K) of 40 W/m.K with a thickness of 1 mm.

To ensure the grid independence of the simulation from the desired mesh, for the simple case of an exchanger with a rigid middle plate, the mesh size has been changed from 1.2 mm to 0.6 and 0.9 mm, and the results can be seen in ***Table 1***. So, we can conclude that the solutions are independent of the size of the mesh.

Table 1. Cold outlet temperature in a simple exchanger with different mesh sizes

Mesh size	Number of elements	The outside temperature
0.6 mm	62230	301.61
0.9 mm	28900	301.59
1.2 mm	17396	301.59

Validation is done with the results of Pirouzfam et al. [22] and shown in ***Figure 4***. Good agreement between results is observed. The average difference between the results of this work and those of Pirouzfam et al. [22] is less than 1%.

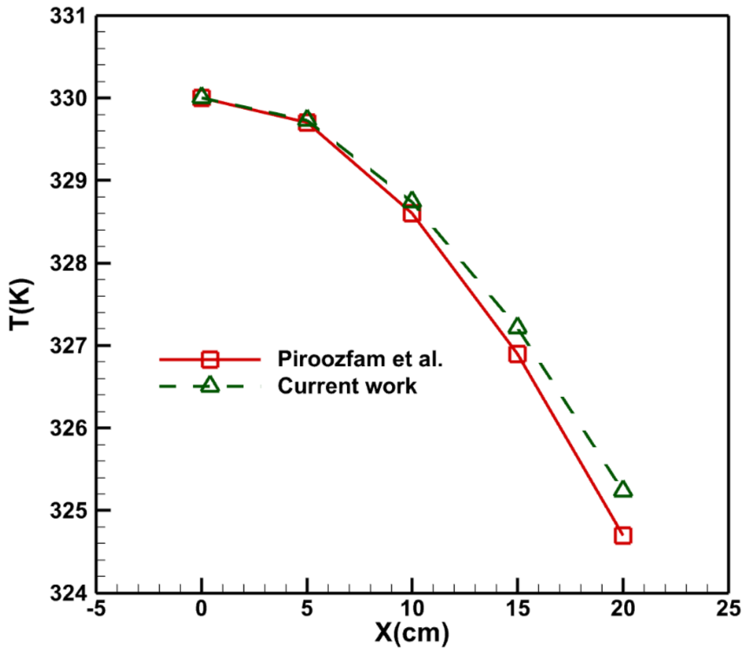

Figure 4. Validation of results (Temperature variation in the channel)

3. Results and discussion

Heat transfer simulation between two fluids has been simulated in COMSOL software with heat transfer models in solids and fluids, solid mechanics, and laminar flow. In the heat transfer model, by defining thermal boundary conditions and initial boundary conditions, heat transfer at different times may vary due to vibration of the elastic part, which causes small disturbances in the fluid and makes heat transfer better. In the solid mechanics model, by defining oscillations with a half-sinusoidal amplitude in the desired sections at different amplitudes and frequencies, we investigate their effect on heat transfer. In the laminar flow model, by introducing boundary conditions and initial conditions, we investigate the fluid flow in the exchanger.

Dimensionless numbers are of particular importance in mechanical engineering research, especially in fluid flow and heat transfer, due to their properties. In heat transfer calculations, the dimensionless form of heat transfer, namely the Nusselt number, is usually used. Therefore, in this section of the present research, the Nusselt number is calculated and displayed under 4 different conditions. In the first one, the elastic plates are in the middle of the heat exchanger and are oscillated uniformly (Mid-Uni). In the second case, the elastic plates are in the middle of the heat exchanger and are oscillated oppositely (Mid-Opp). In the third case, the elastic plates are in the corner of the heat exchanger and are oscillated uniformly (Cor-Uni). In the last case, the elastic plates are in the corner of the heat exchanger and are oscillated oppositely (Cor- Opp). The underlying physical rationale for expecting different performances among these four configurations lies in the interaction between the wall motion and the resulting flow perturbation. Uniform oscillation (Uni) of opposing walls creates a synchronized pumping action, generating coherent, large-scale vortical structures that effectively mix the core flow. In contrast, opposing oscillation (Opp) produces localized counter-moving disturbances that can interfere destructively, limiting the penetration depth of the perturbation into the channel center. Furthermore, the location of the elastic segment—whether in the mid-channel (Mid) or near the corners (Corner)—determines which flow region is primarily affected. Mid-channel oscillation directly targets the high-velocity core, while corner oscillation disrupts the typically stagnant corner flows and shear layers at the wall junctions. The calculated Nusselt number for each case will therefore reflect the combined efficacy of these mechanisms in thinning the thermal boundary layer and enhancing convective heat transfer.

Figure 5 presents the variation of the Nusselt number with oscillation amplitude and frequency for the Mid-Uni configuration. The results conclusively demonstrate the effectiveness of elastic wall oscillation, with all cases exceeding the performance of the traditional rigid-wall exchanger. The Nusselt number enhancement for this setup ranges from 23% to 83%, depending on the specific oscillation parameters. Quantitatively, a 25% increase in amplitude (e.g., from 4 mm to 5 mm) yields an average Nusselt number improvement of 9%, while tripling the frequency from 1 Hz to 3 Hz leads to a more substantial gain of up to 48%. This dominant influence of frequency can be attributed to the fundamental flow mechanics involved: the uniform, in-phase oscillation of the centrally located walls acts as a synchronized pump. This motion periodically accelerates the near-wall fluid, directly disrupting the thermal boundary layer before it can fully develop. Simultaneously, it generates coherent, large-scale vortices that enhance cross-channel mixing between the hot and cold streams. The higher the frequency, the more frequent this cycle of boundary-layer breakdown and bulk fluid agitation becomes, leading to a significantly steeper time-averaged temperature gradient at the wall and, consequently, a higher convective heat transfer rate.

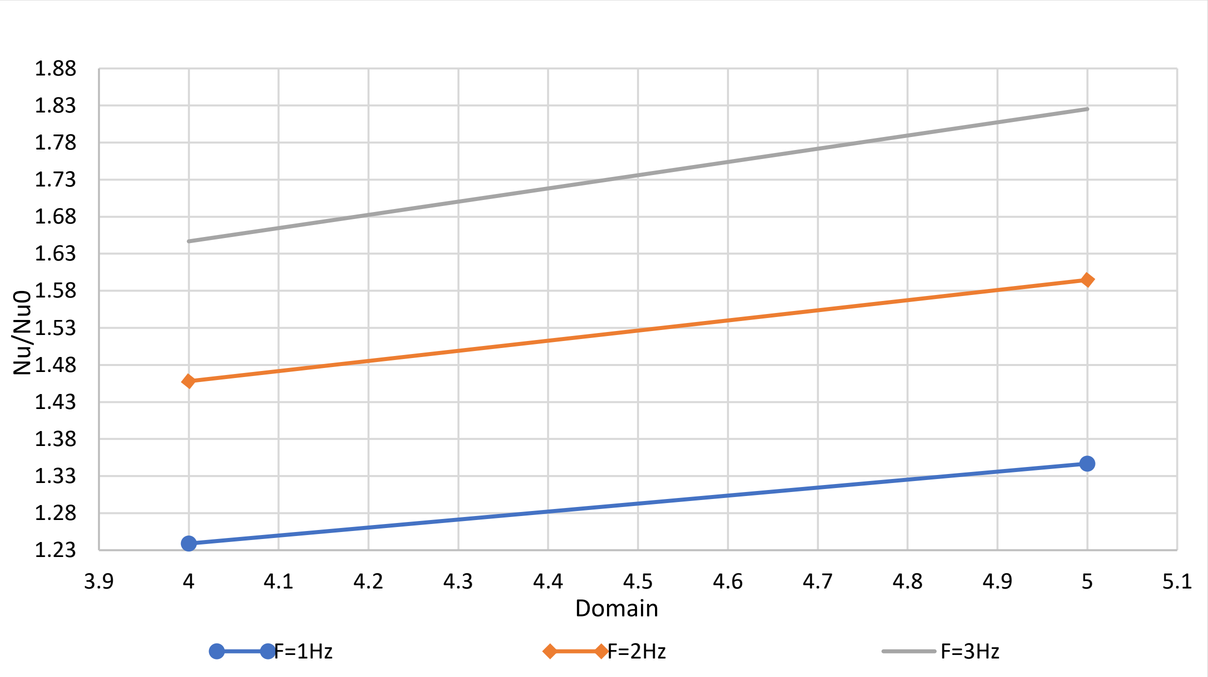

Figure 5. Nusselt number variation with the amplitude and frequency of oscillation (Mid-Uni)

Figure 6 illustrates the impact of oscillation parameters on the Nusselt number for the Mid-Opp configuration. While still outperforming the rigid-wall baseline, the enhancement in this case is more moderate, ranging from 8% to 41%. Parameter sensitivity is also reduced: doubling the oscillation amplitude results in an average Nusselt number increase of only ~5%, and tripling the frequency yields a ~22% improvement. This attenuated performance stems directly from the opposing (out-of-phase) motion of the elastic walls. Instead of generating a unified pumping action, the counter-moving walls create localized flow disturbances that often interfere destructively at the channel centerline. This interference suppresses the formation of the large-scale, coherent vortices observed in the Mid-Uni case, limiting the penetration of momentum and thermal mixing into the core flow region. Consequently, while the thermal boundary layer near each wall is still disturbed, the overall enhancement of convective heat transfer across the entire channel cross-section is less effective.

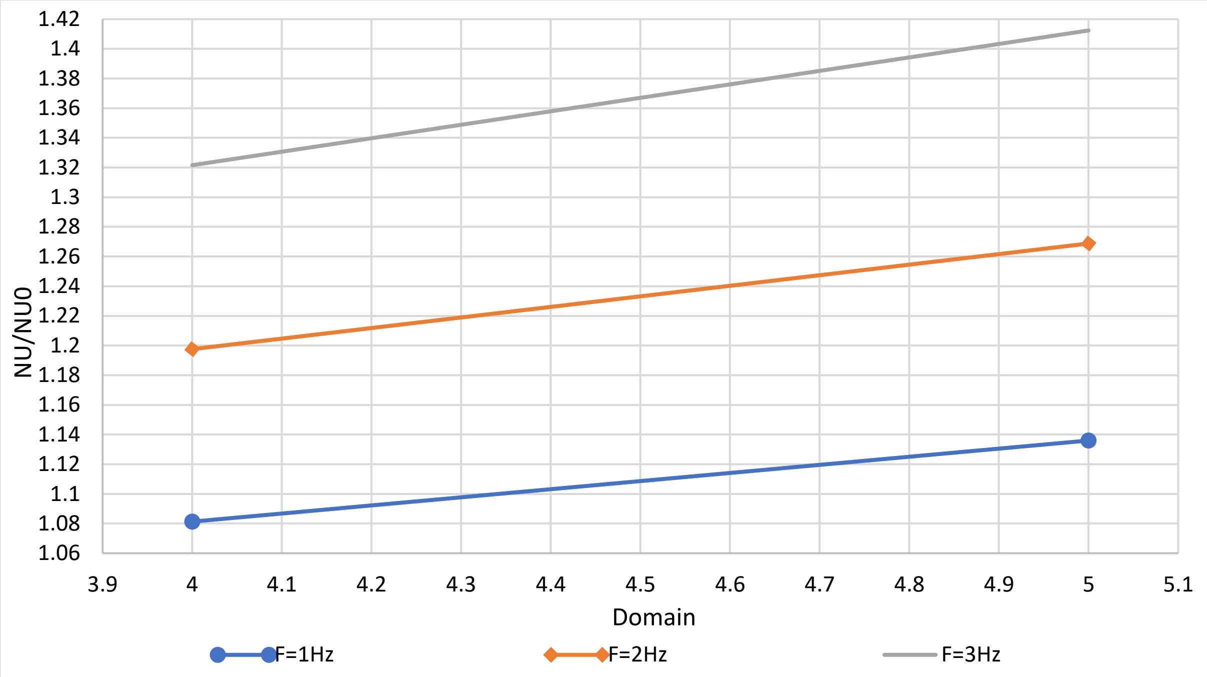

Figure 6. Nusselt number variation with the amplitude and frequency of oscillation (Mid-Opp)

Figure 7 demonstrates the Nusselt number variation for the Cor-Uni configuration. This arrangement yields a remarkable heat transfer enhancement, with Nusselt number increases ranging from 19% to 86%. A key observation is the potent effect of corner placement: increasing the oscillation amplitude from 4 mm to 5 mm (a 25% increase) produces a significant jump in performance. More notably, tripling the oscillation frequency from 1 Hz to 3 Hz boosts the Nusselt number by approximately 39%, reaffirming the dominant role of frequency. The physical mechanism here is distinct and highly effective. Placing the uniformly oscillating walls in the corner regions directly targets the naturally low-velocity, high-thermal-resistance zones where fluid tends to stagnate. The wall motion vigorously agitates this otherwise quiescent fluid, scrubbing away the accumulated thermal boundary layer. Furthermore, the oscillation injects momentum diagonally into the channel, generating strong secondary flow structures that sweep from the corners toward the core, thereby promoting vigorous mixing between the hot and cold streams across a wider portion of the duct. This dual action—corner scrubbing and induced cross-flow—makes the Cor-Uni configuration exceptionally effective.

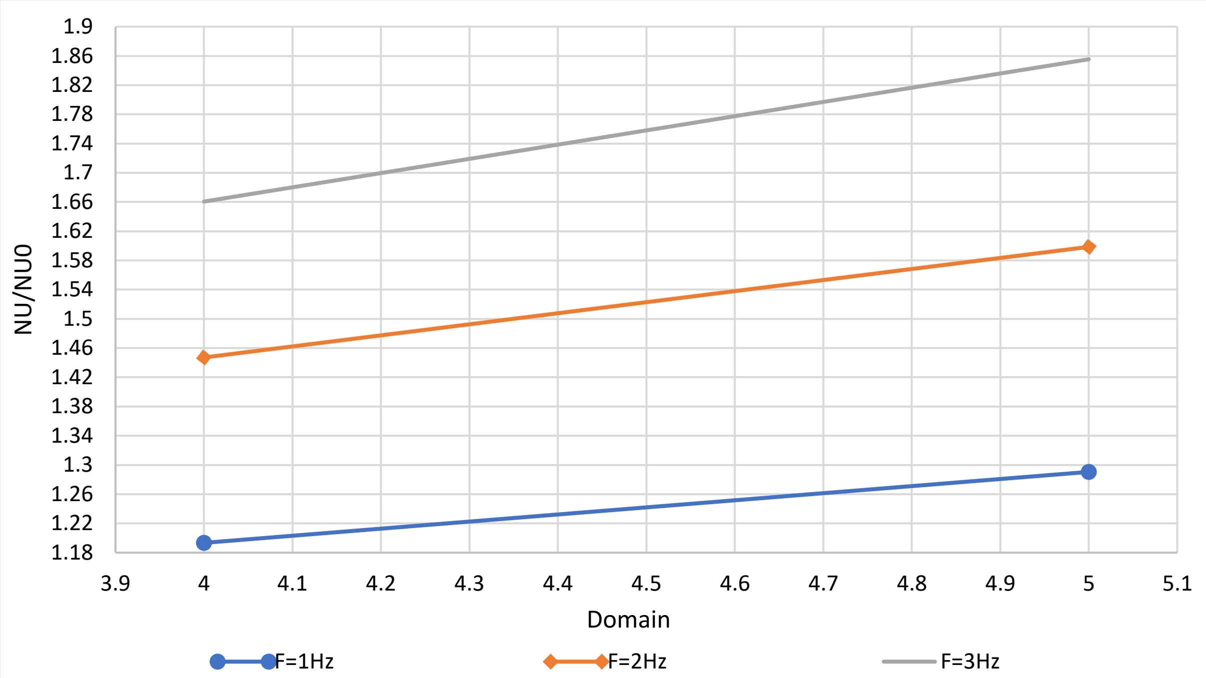

Figure 7. Nusselt number variation with the amplitude and frequency of oscillation (Cor-Mid)

Figure 8 presents the results for the Cor-Opp configuration. This setup provides a substantial heat transfer enhancement, with Nusselt number improvements ranging from 12% to 65% compared to the rigid-wall exchanger. The parameter sensitivity follows a now-familiar pattern: increasing the amplitude from 4 mm to 5 mm results in an average gain of ~7%, while tripling the frequency from 1 Hz to 3 Hz delivers a much more pronounced improvement of ~45%. The physical behavior here is a hybrid of previously explained mechanisms. As with Mid-Opp, the opposing (out-of-phase) oscillation mode limits the synergy between wall motions, preventing the formation of channel-wide coherent flow structures. However, the strategic placement in the corners provides a decisive advantage. Even counter-moving oscillations in these regions are highly effective at disrupting the thick, insulating thermal boundary layers that naturally form in corners. This localized "scrubbing" action forcibly entrains stagnant fluid back into the main flow, leading to a significant recovery of heat transfer potential that would otherwise be lost. Thus, while not as efficient as uniform oscillation, the Cor-Opp configuration still leverages geometric placement to achieve considerable performance gains.

In summary, the analysis of the four configurations reveals two dominant trends. First, oscillation frequency exerts a significantly stronger influence on heat transfer enhancement than oscillation amplitude. Across all cases, tripling the frequency consistently yielded improvements several times greater than those achieved by increasing the amplitude. This underscores the critical role of unsteady inertia and the rate of boundary-layer disruption. Second, both the spatial placement (Mid vs. Corner) and the oscillation mode (Uni vs. Opp) of the elastic walls are paramount in determining the efficiency of flow perturbation. Uniform oscillation (Uni) generates coherent, constructive flow structures that maximize mixing, whereas opposing oscillation (Opp) often leads to partial cancellation of these effects. Meanwhile, corner placement uniquely targets and revitalizes stagnant flow zones. The combination of these factors—frequency, placement, and mode—directly dictates the intensity of thermal boundary layer disruption and the consequent convective heat transfer efficiency.

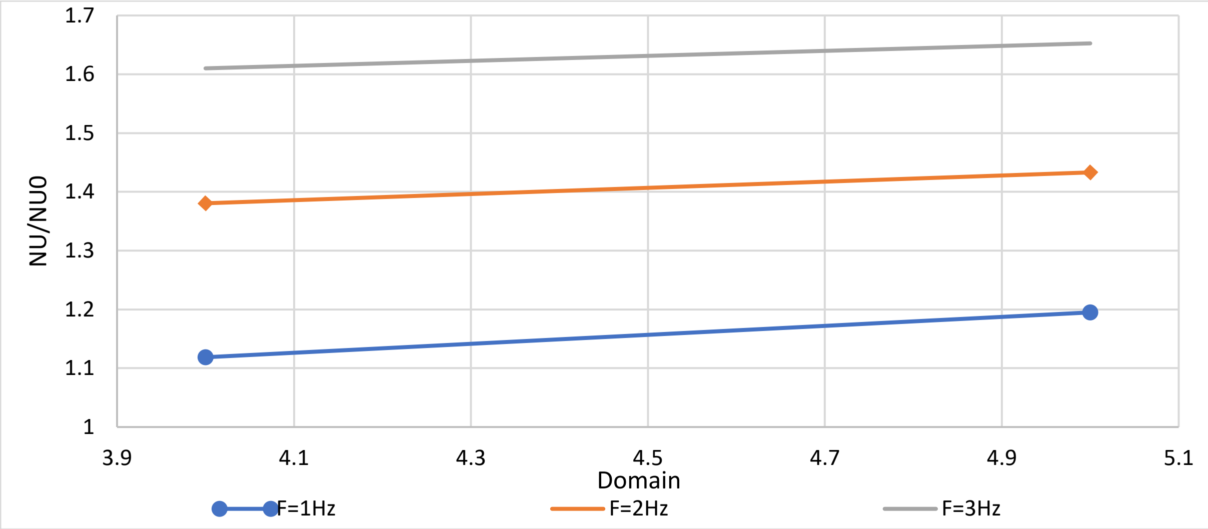

Figure 8. Nusselt number variation with the amplitude and frequency of oscillation (Cor-Mid)

Though the suggested alteration in the heat exchanger led to a significant increase in the Nusselt number, other factors of design, shear stress, pressure drop, and pumping power should also be put into consideration. When using an oscillation-assisted heat exchanger, a higher level of wall motion may amplify the velocity gradient at the wall, and this may result in elevated levels of shear stress. Hence, this section discusses the change in wall shear stress of four configurations that had been studied, as shown in ***Figures 9 to 12***.

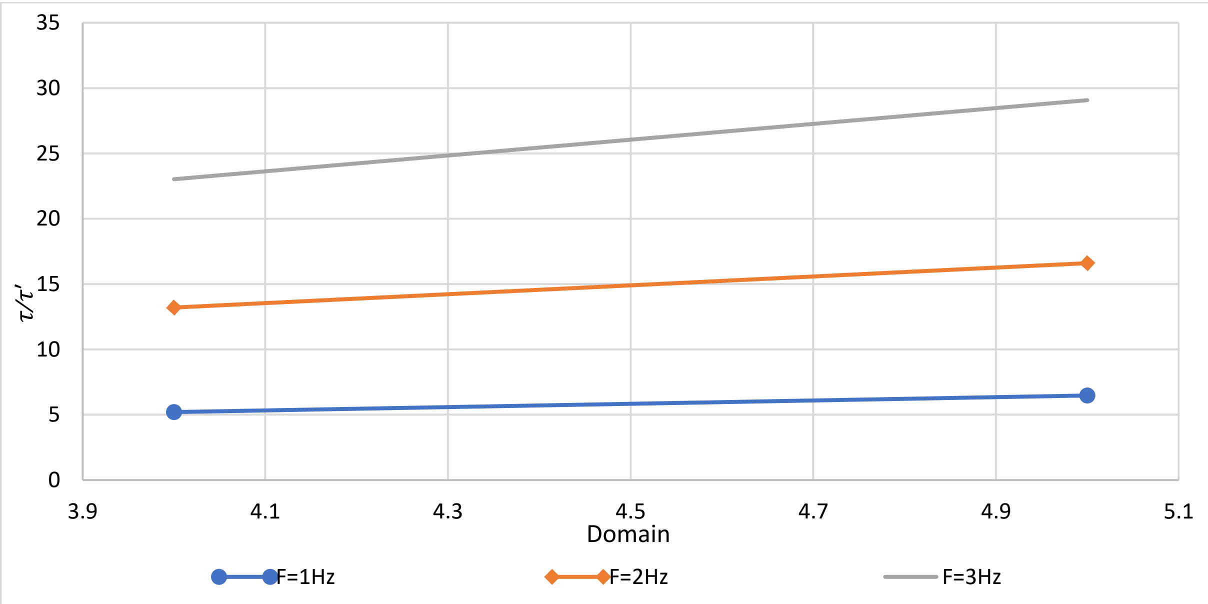

Figure 9. Shear Stress variation with the amplitude and frequency of oscillation (Mid-Uni)

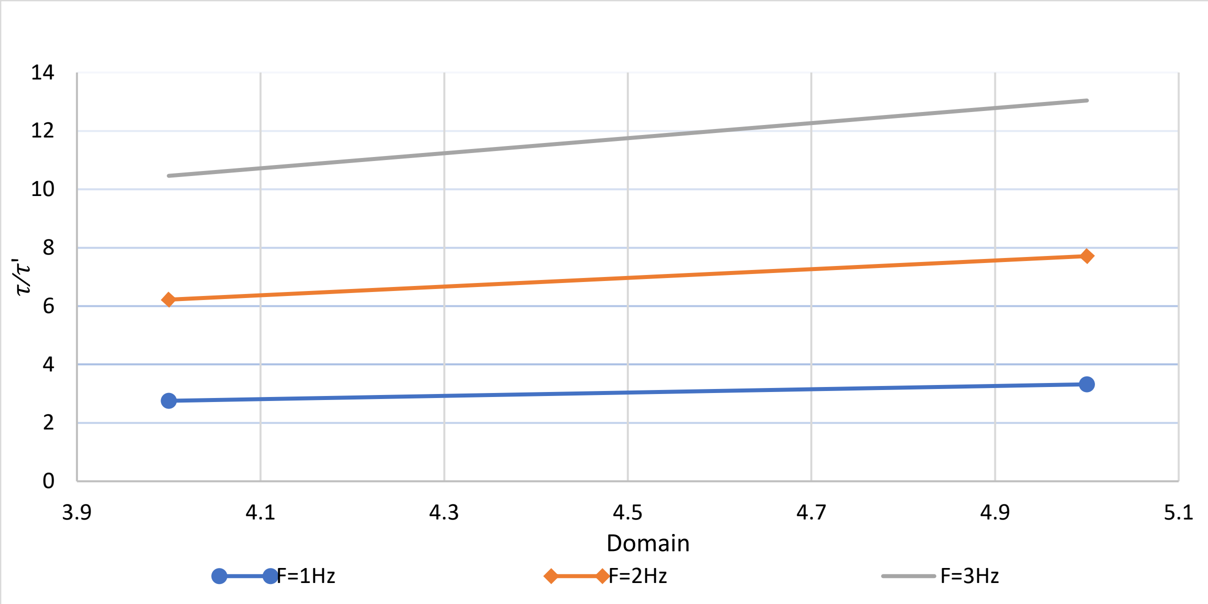

Figure 10. Shear Stress variation with the amplitude and frequency of oscillation (Mid-Opp)

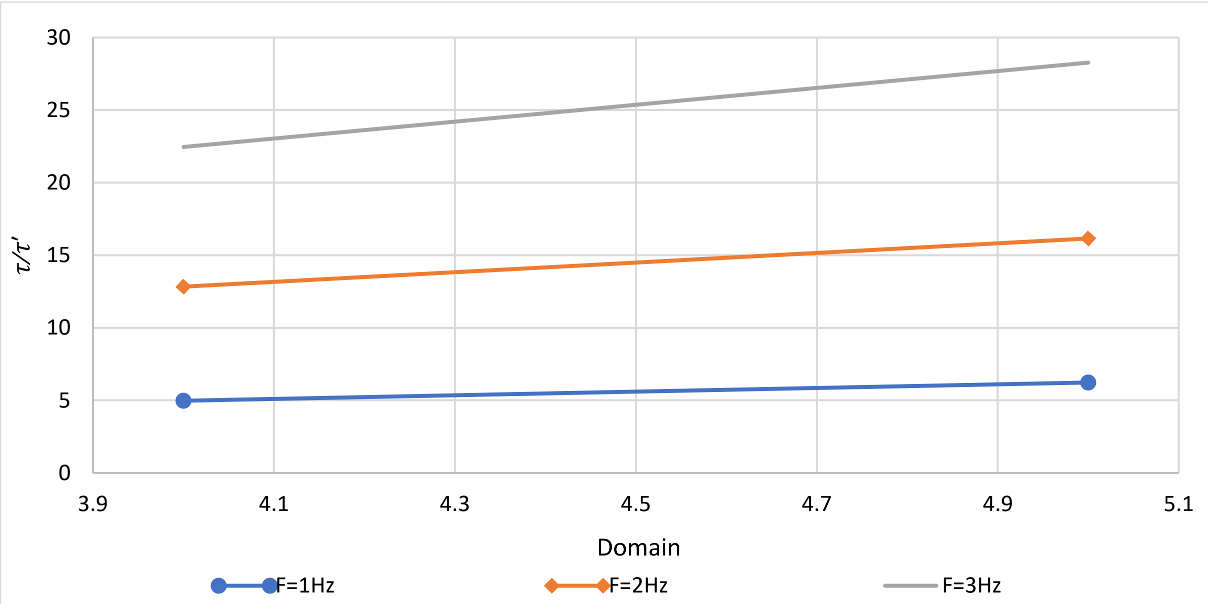

Figure 11. Shear Stress variation with the amplitude and frequency of oscillation (Cor-Uni)

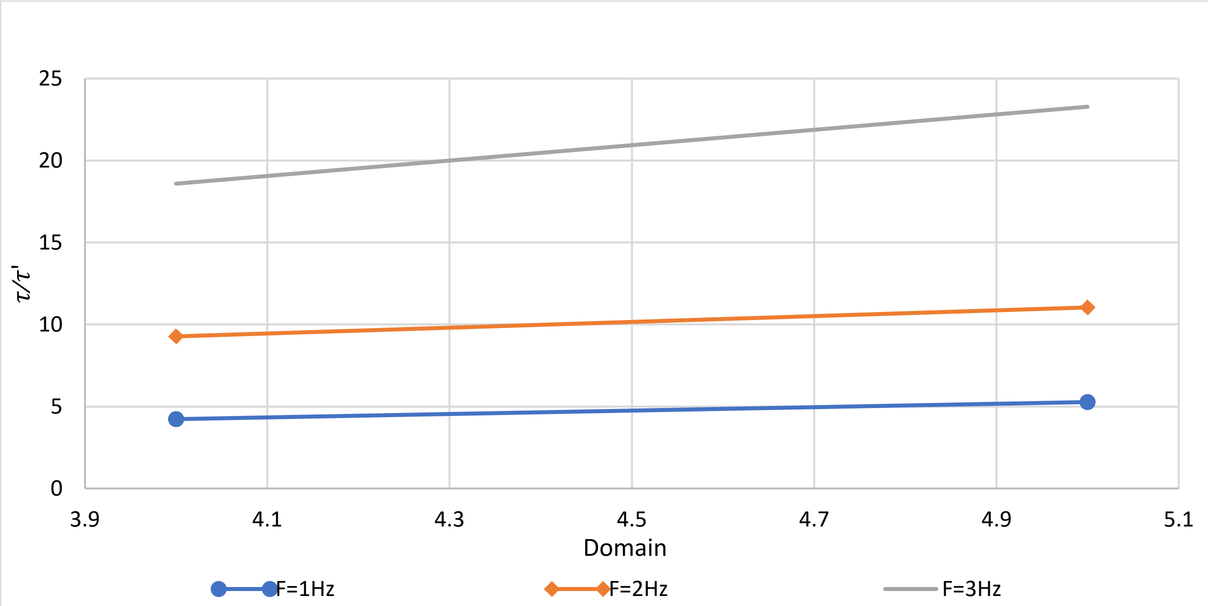

Figure 12. Shear Stress variation with the amplitude and frequency of oscillation (Cor-Opp)

In the case of the Mid-Uni design, when the uniformly oscillating walls are introduced, the shear stress increases significantly, by a factor of between 5 and 29 over a rigid-wall heat exchanger. The average shear stress increases by 24 percent when the amplitude of oscillation is doubled. Moreover, three times the oscillation frequency results in a 4.6-fold increase in the shear stress. The cause of this substantial increase is that the periodic acceleration of the fluid near the vibrating walls is very high and enhances velocity gradients in the viscous sublayer.

The shear stress enhancement is comparatively less in the Mid-Opp setup, and it rises by about 3 to 13 times. An increase in amplitude of oscillation by 25 percent produces an average increase in shear stress by 19%, whereas a tripled frequency increase again produces an increase in shear stress of 4.6 times. The counterbalancing swings to some extent reduce the build-up of near-wall momentum, which causes less shear amplification than in the Mid-Uni case.

In the case of Cor-Uni design, the shear stress is approximately 3 to 12 times higher than that of the simple heat exchanger. An average of a 25% increase in the amplitude of oscillation will increase the shear stress by 20%, and an increase in the oscillation frequency by three times will increase the shear stress by about 4.7 times. The increased shear stress in this arrangement is mainly due to the enhanced acceleration of flow in the corner areas, where oscillatory flow disturbs the stagnant flow areas and flattens the velocity gradients in the vicinity of the walls.

Lastly, in the Cor-Opp design, the shear stress is magnified between 4 and 23 times. Doubling the oscillation amplitude causes the average shear stress to increase by 25%, whereas tripling the oscillation frequency causes an increase in shear stress by 4.4 times. Even though opposing oscillation decreases the coherence of disturbances in walls, the geometric confinement around corners continues to favor the production of intense shear through the localized compression and expansion of streams of flow.

In summary, the numerical investigation yields three overarching conclusions regarding the thermo-hydraulic performance of counter-flow heat exchangers with partly elastic oscillating walls.

First, the addition of oscillating elastic walls substantially enhances convective heat transfer, with Nusselt number improvements ranging from 8% to 86% over the rigid-wall baseline. The highest thermal performance is consistently achieved by uniformly oscillating (Uni) walls, with the Mid-Uni and Cor-Uni configurations being the most effective. This enhancement is physically attributed to the periodic wall motion, which disrupts the thermal boundary layer, induces secondary flows, and promotes vigorous fluid mixing.

Second, this thermal gain is accompanied by a significant hydrodynamic penalty. Wall shear stress is amplified by a factor of 3 to 29, directly indicating increased pressure drops and pumping power requirements. Similar to the heat transfer trend, oscillation frequency is the dominant parameter governing both the enhancement of the Nusselt number and the amplification of shear stress, exerting a far greater influence than oscillation amplitude.

Third, the results reveal a clear performance hierarchy and trade-off. The configuration that delivers the greatest heat transfer (Mid-Uni) also incurs the largest shear stress increase, highlighting an inherent design compromise. performance evaluation criterion (PEC) analysis, however, confirms that all proposed configurations yield a net benefit (PEC > 1), with Mid-Uni achieving the optimal balance.

Therefore, partly elastic oscillating walls represent a promising passive-active enhancement technique. By strategically optimizing the wall placement (Mid vs. Corner), oscillation mode (Uni vs. Opp), and—most critically—the operating frequency, designers can tailor the system to achieve substantial thermal gains while managing the associated hydrodynamic costs, paving the way for next-generation high-efficiency heat exchangers.

Figure 13 gives a comparative analysis of the normalized Nusselt number, which is the ratio of the Nusselt number of the proposed configurations and the base (rigid-wall) Nusselt number, in the four cases under consideration. The configurations that use uniform oscillation always provide higher normalized Nusselt numbers as compared to similar opposite-oscillation configurations, as shown. The trend means that the constant motion of the walls enhances more coherent disturbances in the flow and continued mixing throughout the flow channel, causing more intense disturbance of the thermal boundary layer.

The case of the greatest improvement is Mid-Uni, and the least normalized Nusselt number is observed in the Mid-Opp condition. The decreased efficiency of the Mid-Opp setup is explained by the counter-acting oscillation, which partly nullifies the disturbances caused by the flow and restricts the positive interaction between wall vibration and the core flow. In general, the comparison shows that the oscillation mode is extremely crucial in defining the effectiveness of heat transfer enhancement induced by the elastic-wall.

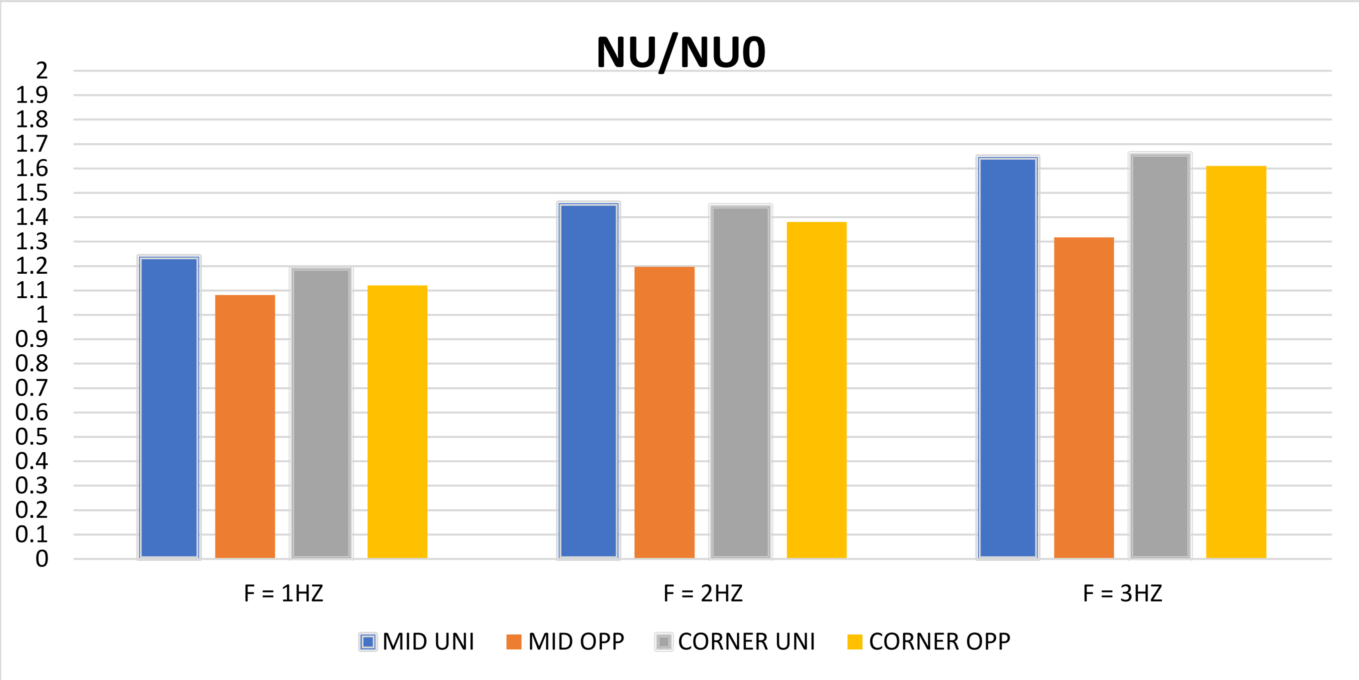

Figure 13. Comparison of Nusselt number in four proposed modes at different frequencies

The performance evaluation criterion (PEC) provides a more comprehensive and balanced evaluation of the heat exchanger's effectiveness. The PEC takes into account both thermal enhancement (via the Nusselt number, Nu) and the associated hydraulic penalty (through the friction factor, f). The PEC is obtained by [23]:

$$\mathrm{PEC} = \frac{\left(\frac{h}{h_0}\right)}{\left(\frac{f}{f_0}\right)^{1/3}} \tag{12}$$

where h is the convective coefficient and f is the friction factor. Any change in the heat exchanger results in new values of h and f, whereas h_0 and f_0 being the baseline values for the heat exchanger. By calculating the PEC for each change, the impact of the change on the heat exchanger performance can be determined. If the PEC is greater than 1, the change is considered beneficial. The PEC is calculated in this work and is shown in ***Figure 14***.

The calculated PEC values, summarized in the accompanying table and illustrated in ***Figure 14***, provide a holistic assessment of the proposed designs by balancing their heat transfer augmentation against the associated hydraulic penalty. A PEC value greater than 1.0 indicates a net beneficial configuration. As the data shows, all configurations with oscillating elastic walls yield PEC values exceeding unity across the tested frequency range (1–5 Hz), confirming their overall superiority over the rigid-wall baseline. The MID UNI configuration consistently achieves the highest PEC, increasing from approximately 1.01 at 1 Hz to 1.28 at 5 Hz. This indicates that the uniform oscillation of centrally located elastic plates not only provides the most significant heat transfer enhancement (as seen in the Nusselt number analysis) but does so with a favorable trade-off against the increased pressure drop, resulting in the best combined thermo-hydraulic performance.

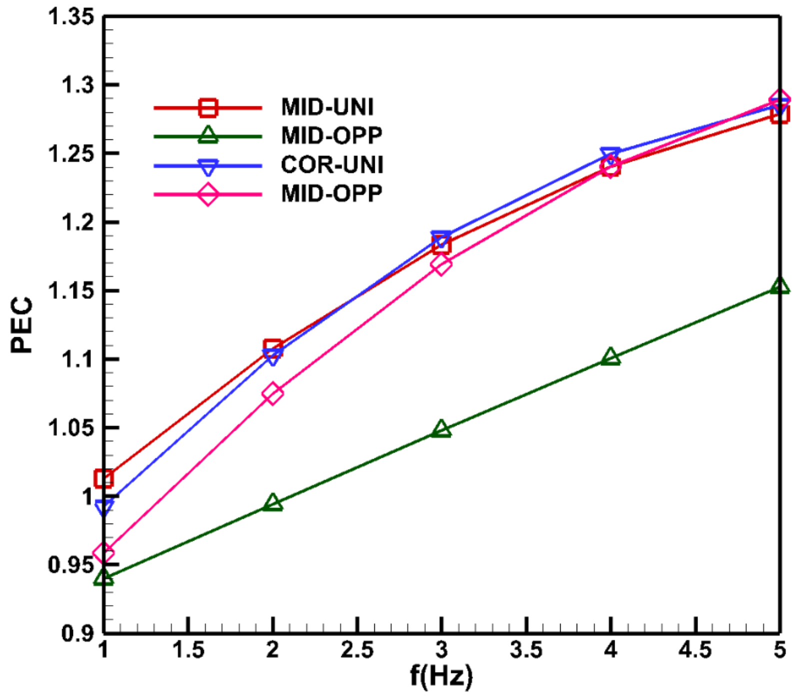

Figure 14. Comparison of PEC in four proposed modes at different frequencies

A clear performance hierarchy is observed: MID UNI > CORNER UNI > CORNER OPP > MID OPP. This order reveals two key trends. First, for a given wall position (middle or corner), the *uniform* oscillation mode (Uni) consistently outperforms the *opposing* mode (Opp). This is because synchronized wall motion creates more coherent, constructive flow disturbances and mixing, whereas opposing motions can partially cancel out these effects, leading to a less efficient conversion of oscillation energy into heat transfer enhancement relative to the incurred friction. Second, for a given oscillation mode, the middle position generally offers a slight advantage over the corner position. Placing elastic walls in the central channel region likely impacts a larger volume of the core flow, promoting more effective overall mixing compared to disturbances generated near the corner boundaries. The progressive rise in PEC with increasing frequency for all cases—particularly the strong improvement in MID UNI—demonstrates that frequency is a critical operational parameter for optimizing system efficiency. These PEC results substantiate the central finding of this study: incorporating partly elastic, oscillating walls is a strategically viable method for enhancing counter-flow heat exchanger performance. The MID UNI configuration emerges as the most recommendable design, successfully leveraging controlled wall oscillation to disrupt thermal boundary layers and enhance mixing, while maintaining an efficient balance between thermal gain and pumping power cost across the operational range.

The results of the current paper indicate that counter-flow heat exchangers with partially elastic and vibrating intermediate walls can provide a viable and efficient method of increasing thermal performance in a large spectrum of industrial applications. The high Nusselt number, which is realized in the suggested configurations, implies there is a high potential of application in compact heat exchangers, condensers, evaporators, and thermal management systems where high heat transfer rates are expected to be achieved within a limited space. These designs can also prove beneficial in processes that consume a lot of energy, such as chemical processing, HVAC, waste heat recovery, and desalination plants, where better thermal efficiency can simply be converted into lower energy use and lower operational cost.

Engineering-wise, the capability of adjusting the performance of heat transfer by means of controlled elastic wall oscillation gives an extra degree of freedom to the heat exchanger design. That is, optimization of thermal enhancement can be achieved by controlling the oscillation frequency, amplitude, and wall placement, and controlling hydrodynamic penalties like higher shear stress and pumping power. This flexibility also contributes to the elastic-wall heat exchanger with oscillating walls being especially appealing to use in applications where some adaptive or load-dependent thermal control is needed.

The next research direction would be to apply the current numerical framework to three-dimensional geometries and the turbulent flow regimes to further determine the scalability of the idea presented. The predicted trends of thermal and hydrodynamic behavior should also be checked by experimental validation to ascertain the long-term oscillatory behavior of materials and to determine their durability. Additionally, the smart actuation and control strategies, including adaptive oscillation using real-time thermal demand, might also enhance the efficiency and reliability of the system. These research directions will facilitate the gap between numerical modeling and industrial application of elastic-wall-assisted heat exchangers.

4. Conclusion

This paper has numerically analyzed a counter-flow plate heat exchanger fitted with partially elastic intermediate walls to analyze its thermal and hydrodynamic performance through a fluid-structure interaction framework. The findings show that the addition of oscillating elastic walls results in a significant increase in heat transfer when compared to a standard rigid-wall heat exchanger. The Nusselt number was enhanced by about 8-86% depending on the position of the elastic wall and mode of oscillation, with the greatest improvement of the elastic plates noted when the plates were placed in the central section and vibrated in the same way. A three-fold rise in oscillation rate caused a maximum 48% rise in the Nusselt number, and a 25 per cent rise in oscillation amplitude caused an average 5-9% improvement in heat transfer efficiency. The increase in heat transfer was, however, coupled with a significant increase in shear stress, a point that reflects a trade-off between thermal and hydrodynamic penalties. The performance evaluation criterion (PEC) analysis confirms that all oscillating-wall configurations are beneficial, with values ranging from 0.94 (indicating a borderline case for MID OPP at the lowest frequency) to a maximum of 1.29 (achieved by MID UNI at the highest frequency). The clear performance hierarchy—MID UNI > CORNER UNI > CORNER OPP > MID OPP—demonstrates that uniform oscillation and central wall placement yield the optimal balance between heat transfer augmentation and pressure drop. The significant increase in PEC with frequency, culminating in the 1.29 value, underscores the effectiveness of controlled high-frequency wall oscillation as a superior strategy for enhancing thermo-hydraulic performance in counter-flow heat exchangers.

The work in the future can be to optimize elastic wall materials and geometries such that pressure losses are minimized without compromising the high heat transfer rates. It is also suggested to extend the current model to turbulent flow regimes, three-dimensional geometries, and variable fluid properties. Furthermore, the elastic-wall ideas and integration with smart control schemes could be further experimentally processed and prove the practicality of the implementation of oscillating elastic heat exchangers in industrial systems.

References

[1] Careri, F., Khan, R. H. U., Todd, C., & Attallah, M. M. (2023). Additive manufacturing of heat exchangers in aerospace applications: A review. *Applied Thermal Engineering*, *235*, 121387.

[2] Bretado-de los Rios, M. S., Rivera-Solorio, C. I., & Nigam, K. D. P. (2021). An overview of sustainability of heat exchangers and solar thermal applications with nanofluids: A review. *Renewable and Sustainable Energy Reviews*, *142*, 110855.

[3] Razavi, S. E., Adibi, T., Halool Abohned, M. N., Ahmed, S. F., & Alotaibi, H. (2025). Performance optimization of Maisotsenko cycle heat exchangers: A three-dimensional parametric analysis. *Case Studies in Thermal Engineering*, 105829.

[4] Lahmer, D., Benamara, N., Ahmad, H., Ameur, H., & Boulenouar, A. (2022). Combination of the parallel/counter flows nanofluid techniques to improve the performances of double-tube thermal exchangers. *Arabian Journal for Science and Engineering*, *47*(6), 7789–7796.

[5] Bartecki, K. (2021). An approximate transfer function model for a double-pipe counter-flow heat exchanger. *Energies*, *14*(14), 4174.

[6] Stehlík, P., & Wadekar, V. V. (2002). Different strategies to improve industrial heat exchange. *Heat Transfer Engineering*, *23*(6), 36–48.

[7] Gerken, I., Wetzel, T., & Brandner, J. J. (2021). Efficiency improvement of miniaturized heat exchangers. *Fluids*, *6*(1), 25.

[8] Shahrukh Khan, L., Hafiz Khawar, H., & Ibrar, H. (2024). Using AI to increase heat exchanger efficiency: An extensive analysis of innovations and uses. *International Journal of Multidisciplinary Sciences and Arts*, *3*(4), 1–14.

[9] Osintsev, K., Aliukov, S., Kuskarbekova, S., Tarasova, T., Karelin, A., Konchakov, V., & Kornyakova, O. (2023). Increasing thermal efficiency: Methods, case studies, and integration of heat exchangers with renewable energy sources and heat pumps for desalination. *Energies*, *16*(13), 4930.

[10] K, N. V. (2024). Opportunities, challenges, and state of the art of flexible heat-pipe heat exchangers: A comprehensive review. *Heat Transfer*, *53*(2), 893–938.

[11] Bhattacharyya, S., Vishwakarma, D. K., Srinivasan, A., Soni, M. K., Goel, V., Sharifpur, M., ... & Meyer, J. (2022). Thermal performance enhancement in heat exchangers using active and passive techniques: a detailed review. *Journal of Thermal Analysis and Calorimetry*, *147*(17), 9229-9281.

[12] Adibi, T., Razavi, S. E., Ahmed, S. F., Shakor, M. M., & Liu, G. (2024). Effects of elastic walls on the thermal performance of a counterflow heat exchanger. *International Journal of Energy Research*, *2024*(1), 8895936.

[13] Ji, J., Lu, Y., Shi, B., Gao, R., & Chen, Q. (2023). Numerical research on vibration and heat transfer performance of a conical spiral elastic bundle heat exchanger with baffles. *Applied Thermal Engineering*, *232*, 121036.

[14] Ji, J., Gao, R., Shi, B., Zhang, J., Li, F., & Deng, X. (2022). Improved tube structure and segmental baffle to enhance heat transfer performance of elastic tube bundle heat exchanger. *Applied Thermal Engineering*, *200*, 117703.

[15] Ji, J., Ni, X., Shi, B., Pan, Y., & Liu, P. (2024). Influence of deflector direction on heat transfer capacity of spiral elastic tube heat exchanger. *Applied Thermal Engineering*, *236*, 121754.

[16] Afridi, M. I., Pourahmad, S., Maleki, N. M., Tavousi, E., Rahbari, A., Adibi, T., & Sharifpur, M. (2026). Experimental examination of thermohydraulic characteristics of a new vibrating rubber tube turbulator with multiple air bubble outlets inserted inside a double-pipe heat exchanger. *International Communications in Heat and Mass Transfer*, *172*, 110509.

[17] Adibi, T., Maleki, N. M., Tavousi, E., & Keshmiri, A. (2025). Enhancing the heat transfer efficiency in heated tube with a novel multi-twisted blade turbulators: A numerical analysis. *International Communications in Heat and Mass Transfer*, *169*, 109717.

[18] Xu, Z., Wang, J., Zhang, L., Sun, H., Li, M., & Campbell, J. (2022). Study on thermal deformation of hybrid printed circuit heat exchanger for advanced nuclear reactor. *Cleaner Energy Systems*, *3*, 100025.

[19] Razavi, S. E., Adibi, T., Abohned, M. N. H., Ahmed, S. F., & Alotaibi, H. (2025). Performance optimization of Maisotsenko cycle heat exchangers: A three-dimensional parametric analysis. *Case Studies in Thermal Engineering*, *67*, 105829.

[20] Ji, J., Pan, Y., Zhang, J., Shi, B., & Bao, L. (2024). Numerical study on the effect of baffle structure on the heat transfer performance of elastic tube bundle heat exchanger. *Applied Thermal Engineering*, *238*, 122220.

[21] Adibi, T., & Razavi, S. E. (2015). A new characteristic approach for incompressible thermo-flow in Cartesian and non-Cartesian grids. *International Journal for Numerical Methods in Fluids*, *79*(8), 371–393.

[22] Piroozfam, N., Hosseinpour Shafaghi, A., & Razavi, S. E. (2018). Numerical investigation of three methods for improving heat transfer in counter-flow heat exchangers. *International Journal of Thermal Sciences, 133,* 230–239.

[23] Razavi, S. E., & Hassanpour, H. (2021). Thermo-flow analysis of cylinder with crossed splitter plates with a characteristics-based scheme. *International Journal of Thermodynamics*, *24*(2), 83–91.